

A Transmission Problem in Electromagnetism with a Singular Interface

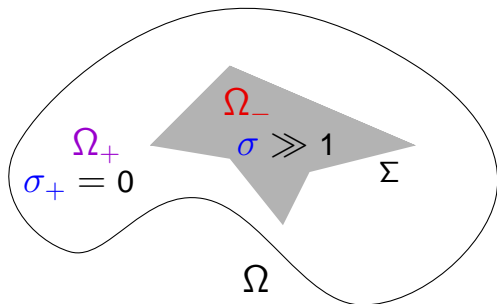
GABRIEL CALOZ² MONIQUE DAUGE² ERWAN FAOU² V. PÉRON¹
CLAIR POIGNARD¹

¹ Projet MC2, INRIA Bordeaux Sud-Ouest

² IRMAR, Université de Rennes 1

6th Singular Days on Asymptotic Methods for PDEs
WIAS Berlin, April 29 – May 1, 2010

The Skin Effect : A Model Problem



- Ω_- Highly Conducting body $\subset\subset \Omega$: Conductivity $\sigma_- \equiv \sigma \gg 1$
- $\Sigma = \partial\Omega_-$: Interface
- Ω_+ Insulating or Dielectric body: Conductivity $\sigma_+ = 0$

The **Skin Effect**: rapid decay of electromagnetic fields with depth inside the conductor.

The **Skin Depth**: $\ell(\sigma) = \sqrt{2/\omega\mu_0\sigma}$

References



V. PÉRON (PhD 09)



G. CALOZ, M. DAUGE, V. PÉRON (JMAA 10)

Uniform Estimates for Transmission Problems with High Contrast in Heat Conduction and Electromagnetism



M. DAUGE, E. FAOU, V. PÉRON (CRAS 10)

Asymptotic Behavior for High Conductivity of the Skin Depth Electromagnetism

- Aim : Understanding the influence of the geometry of a conducting body on the skin effect in electromagnetism.

Outline

- 1 Framework
- 2 3D Multiscaled Asymptotic Expansion
- 3 Axisymmetric Problems
- 4 Finite Element Computations
- 5 Numerical simulations of skin effect
- 6 Postprocessing

Outline

- 1 **Framework**
- 2 3D Multiscaled Asymptotic Expansion
- 3 Axisymmetric Problems
- 4 Finite Element Computations
- 5 Numerical simulations of skin effect
- 6 Postprocessing

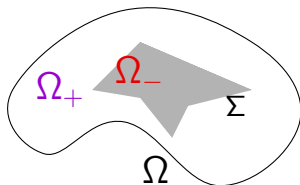
Framework

Maxwell Problem

$$(\mathbf{P}_{\underline{\sigma}}) \quad \operatorname{curl} \mathbf{E} - i\omega\mu_0 \mathbf{H} = 0 \quad \text{and} \quad \operatorname{curl} \mathbf{H} + (i\omega\varepsilon_0 - \underline{\sigma}) \mathbf{E} = \mathbf{j}$$

$$\underline{\sigma} = (0, \sigma \gg 1)$$

$$\mathbf{j} \in \mathbf{H}_0(\operatorname{div}, \Omega) = \{\mathbf{u} \in \mathbf{L}^2(\Omega) \mid \operatorname{div} \mathbf{u} \in L^2(\Omega), \mathbf{u} \cdot \mathbf{n} = 0 \text{ on } \partial\Omega\}$$



Perfectly Conducting Magnetic Wall B. C.:

$$\mathbf{E} \cdot \mathbf{n} = 0 \quad \text{and} \quad \mathbf{H} \times \mathbf{n} = 0 \quad \text{on} \quad \partial\Omega$$

Existence of solutions

Hypothesis (SH)

The angular frequency ω is not an eigenfrequency of the problem

$$\left\{ \begin{array}{ll} \operatorname{curl} \mathbf{E} - i\omega\mu_0 \mathbf{H} = 0 & \text{and } \operatorname{curl} \mathbf{H} + i\omega\varepsilon_0 \mathbf{E} = 0 & \text{in } \Omega_+ \\ \mathbf{E} \times \mathbf{n} = 0 & & \text{on } \Sigma \\ \text{B.C.} & & \text{on } \partial\Omega \end{array} \right.$$

Theorem (CALOZ, DAUGE, P., 09)

If the surface Σ is Lipschitz, under Hypothesis (SH), there exist σ_0 and $C > 0$, such that for all $\sigma \geq \sigma_0$, (\mathbf{P}_σ) with B.C. and $\mathbf{j} \in \mathbf{H}(\operatorname{div}, \Omega)$ has a unique solution (\mathbf{E}, \mathbf{H}) in $L^2(\Omega)^2$, and

$$\|\mathbf{E}\|_{0,\Omega} + \|\mathbf{H}\|_{0,\Omega} + \sqrt{\sigma} \|\mathbf{E}\|_{0,\Omega_-} \leq C \|\mathbf{j}\|_{\mathbf{H}(\operatorname{div}, \Omega)}$$

Application: Convergence of asymptotic expansion for large conductivity

Outline

- 1 Framework
- 2 3D Multiscaled Asymptotic Expansion**
- 3 Axisymmetric Problems
- 4 Finite Element Computations
- 5 Numerical simulations of skin effect
- 6 Postprocessing

References and Notations

Asymptotic Expansion as $\sigma \rightarrow \infty$ of solutions of (\mathbf{P}_σ) when Σ is smooth :



E.P. STEPHAN, R.C. MCCAMY (83-84-85)

Plane Interface and Eddy Current Problems



H. HADDAR, P. JOLY, H.N. NGUYEN (08)

Generalized Impedance Boundary Conditions



G. CALOZ, M. DAUGE, V. PÉRON (JMAA 10)



M. DAUGE, E. FAOU, V. PÉRON (CRAS 10)



PÉRON (09)

Hypothesis

- 1 Σ is a Smooth Surface
- 2 ω satisfies the Spectral Hypothesis (SH)
- 3 \mathbf{j} is smooth and $\mathbf{j} = 0$ in Ω_-

Asymptotic Expansion

$$\delta := \sqrt{\omega \varepsilon_0 / \sigma} \longrightarrow 0 \quad \text{as} \quad \sigma \rightarrow \infty$$

By Theorem there exists δ_0 s.t. for all $\delta \leq \delta_0$, the solution $\mathbf{H}(\delta)$ to (\mathbf{P}_σ) :

$$\mathbf{H}_{(\delta)}^+(\mathbf{x}) \approx \mathbf{H}_0^+(\mathbf{x}) + \delta \mathbf{H}_1^+(\mathbf{x}) + \mathcal{O}(\delta^2)$$

$$\mathbf{H}_{(\delta)}^-(\mathbf{x}) \approx \mathbf{H}_0^-(\mathbf{x}; \delta) + \delta \mathbf{H}_1^-(\mathbf{x}; \delta) + \mathcal{O}(\delta^2)$$

$$\text{with} \quad \mathbf{H}_j^-(\mathbf{x}; \delta) = \chi(y_3) \mathbf{V}_j(y_\beta, \frac{y_3}{\delta}).$$

(y_β, y_3) : “*normal coordinates*” to Σ in a tubular region \mathcal{U}_- of Σ in Ω_-

$\mathbf{H}_j^+ \in \mathbf{H}(\text{curl}, \Omega_+)$ and $\mathbf{V}_j \in \mathbf{H}(\text{curl}, \Sigma \times \mathbb{R}_+)$ *profiles*.

$$\|\mathbf{H}_j^-(\mathbf{x}; \delta)\|_{0, \Omega_-} \leq C_j \sqrt{\delta} \quad \text{for all} \quad j \in \mathbb{N}$$

Profiles of the Magnetic Field

$\mathbf{v}_j =: (\mathcal{V}_j^\alpha; v_j)$ in coordinates (y_β, Y_3) with $Y_3 = \frac{y_3}{\delta}$

$$\mathbf{v}_0(y_\beta, Y_3) = \mathbf{h}_0(y_\beta) e^{-\lambda Y_3}$$

$$\mathcal{V}_1^\alpha(y_\beta, Y_3) = \left[h_1^\alpha + Y_3 \left(\mathcal{H} h_0^\alpha + b_\sigma^\alpha h_0^\sigma \right) \right] (y_\beta) e^{-\lambda Y_3}$$

Here,

\mathcal{H} mean curvature of Σ

$$\mathbf{h}_0(y_\beta) = (\mathbf{n} \times \mathbf{H}_0^+) \times \mathbf{n}(y_\beta, 0) \quad \text{and} \quad h_j^\alpha(y_\beta) := (\mathbf{H}_j^+)^\alpha(y_\beta, 0)$$

$$\lambda = \omega \sqrt{\varepsilon_0 \mu_0} e^{-i\pi/4}$$

Application

A New Definition of the Skin Depth

$$\mathbf{v}_{(\delta)}(y_\alpha, y_3) := \mathbf{H}_{(\delta)}^-(\mathbf{x}), \quad y_\alpha \in \Sigma, \quad 0 \leq y_3 < h_0$$

Definition

Let Σ be a smooth surface, and \mathbf{j} s.t. $\mathbf{v}_{(\delta)}(y_\alpha, 0) \neq 0$. The skin depth is the smallest length $\mathcal{L}(\sigma, y_\alpha)$ defined on Σ s.t.

$$\|\mathbf{v}_{(\delta)}(y_\alpha, \mathcal{L}(\sigma, y_\alpha))\| = \|\mathbf{v}_{(\delta)}(y_\alpha, 0)\| e^{-1}$$

Theorem (DAUGE, FAOU, P., 10)

Let Σ be a regular surface with mean curvature \mathcal{H} , and assume $\mathbf{h}_0(y_\alpha) \neq 0$.

$$\mathcal{L}(\sigma, y_\alpha) = \ell(\sigma) \left(1 + \mathcal{H}(y_\alpha) \ell(\sigma) + \mathcal{O}(\sigma^{-1}) \right), \quad \sigma \rightarrow \infty$$

Key of the proof:

$$\|\mathbf{v}_{(\delta)}\|^2 = \left[\|\mathbf{h}_0\|^2 + 2y_3 \mathcal{H} \|\mathbf{h}_0\|^2 + 2\delta \operatorname{Re}\langle \mathbf{h}_0, \mathbf{h}_1 \rangle + \mathcal{O}((\delta + y_3)^2) \right] e^{-2y_3/\ell(\sigma)}$$

Outline

- 1 Framework
- 2 3D Multiscaled Asymptotic Expansion
- 3 Axisymmetric Problems**
- 4 Finite Element Computations
- 5 Numerical simulations of skin effect
- 6 Postprocessing

Axisymmetric domains

The meridian domain

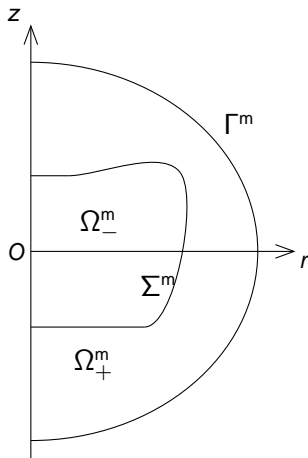


Figure: The meridian domain $\Omega^m = \Omega_-^m \cup \Omega_+^m \cup \Sigma^m$

Reduction problem

$$\begin{cases} (\operatorname{curl} \mathbf{H})_r = \frac{1}{r} \partial_\theta H_z - \partial_z H_\theta, \\ (\operatorname{curl} \mathbf{H})_\theta = \partial_z H_r - \partial_r H_z, \\ (\operatorname{curl} \mathbf{H})_z = \frac{1}{r} (\partial_r (r H_\theta) - \partial_\theta H_r). \end{cases}$$

The Maxwell problem is axisymmetric : the coefficients do not depend on the angular variable θ .

Reduction problem

$$\begin{cases} (\operatorname{curl} \mathbf{H})_r = \frac{1}{r} \partial_\theta H_z - \partial_z H_\theta, \\ (\operatorname{curl} \mathbf{H})_\theta = \partial_z H_r - \partial_r H_z, \\ (\operatorname{curl} \mathbf{H})_z = \frac{1}{r} (\partial_r (r H_\theta) - \partial_\theta H_r). \end{cases}$$

The Maxwell problem is axisymmetric : the coefficients do not depend on the angular variable θ .

\mathbf{H} is axisymmetric iff $\check{\mathbf{H}} := (H_r, H_\theta, H_z)$ does not depend on θ .

Assume that the right-hand side is axisymmetric and orthoradial. Then, $\mathbf{H}_{(\delta)}$ is axisymmetric and orthoradial :

$$\check{\mathbf{H}}_{(\delta)}(r, \theta, z) = (0, h_{(\delta)}(r, z), 0).$$

Configurations chosen for computations

Configuration A

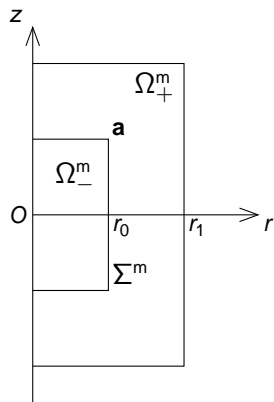


Figure: The meridian domain Ω^m in configuration A

Configurations chosen for computations

Configuration B

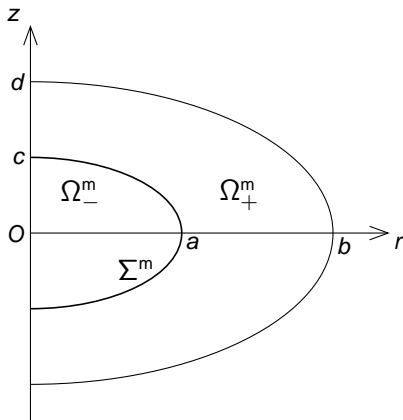


Figure: The meridian domain Ω^m in configuration B

Outline

- 1 Framework
- 2 3D Multiscaled Asymptotic Expansion
- 3 Axisymmetric Problems
- 4 Finite Element Computations**
- 5 Numerical simulations of skin effect
- 6 Postprocessing

Finite Element Method

- High order elements available in the finite element library MéliNa
- $h_{(\delta)}^{\rho, \mathfrak{M}}$: the computed solution of the discretized problem with an interpolation degree ρ and a mesh \mathfrak{M}

$$A_{\sigma}^{\rho, \mathfrak{M}} := \|h_{(\delta)}^{\rho, \mathfrak{M}}\|_{L_1^2(\Omega_-^m)} \quad \text{with} \quad \sigma = \omega \varepsilon_0 \delta^{-2}$$

$$\|v\|_{L_1^2(\Omega_-^m)}^2 = \int_{\Omega_-^m} |v|^2 r dr dz .$$

- In the computations, the angular frequency $\omega = 3.10^7$.

Interpolation degree

Configuration B

We first check the convergence when the interpolation degree p of the finite elements increases.

We consider the discretized problem with different degrees: Q_p , $p = 1, \dots, 20$, and with 2 different meshes:

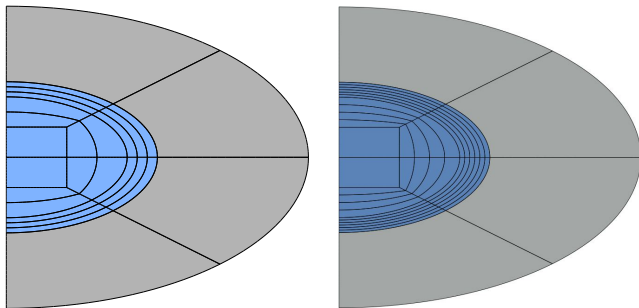
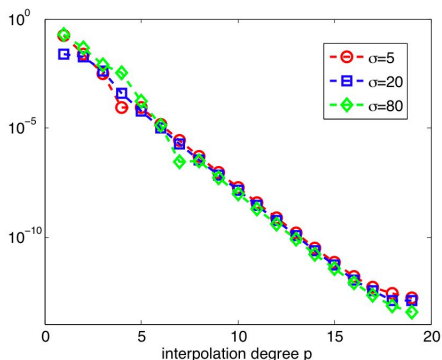


Figure: The meshes \mathfrak{M}_3 and \mathfrak{M}_6

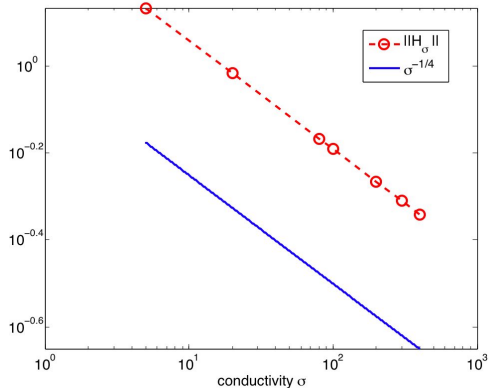
We represent the absolute value of the difference between the weighted norms $A_{\sigma}^{\rho, \mathcal{M}_3}$ and $A_{\sigma}^{20, \mathcal{M}_6}$, versus p in semilogarithmic coordinates



SCHWAB, SURI (96)

theoretical results of convergence for the p-version of problems with boundary layers

We plot in log-log coordinates the weighted norm $A_{\sigma}^{16, \mathcal{M}_3}$ with respect to σ with red circles.



The figure shows that $A_{\sigma}^{16, \mathcal{M}_3}$ behaves like $\sigma^{-1/4}$ (solid line) when $\sigma \rightarrow \infty$. This behavior is consistent with the asymptotic expansion.

Configuration A

We consider a family of meshes with square elements \mathfrak{M}_k , with size $h = 1/k$

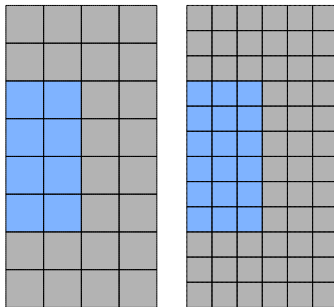
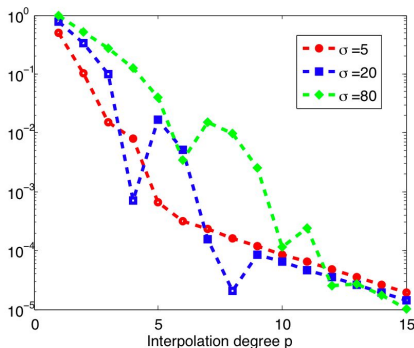


Figure: Meshes \mathfrak{M}_2 , and \mathfrak{M}_3 in configuration A

Configuration A

We represent the absolute value of the difference between $A_\sigma^{\rho, \mathfrak{M}_2}$ and $A_\sigma^{16, \mathfrak{M}_3}$, versus ρ in semilogarithmic coordinates



The figure shows that $A_\sigma^{\rho, \mathfrak{M}_2}$ approximates $A_\sigma^{16, \mathfrak{M}_3}$ better than 10^{-4} when $\rho \geq 12$.

Outline

- 1 Framework
- 2 3D Multiscaled Asymptotic Expansion
- 3 Axisymmetric Problems
- 4 Finite Element Computations
- 5 Numerical simulations of skin effect**
- 6 Postprocessing

Skin effect in configuration B

$$|\operatorname{Im} h_{(\delta)}^+| = \mathcal{O}(\delta).$$

Thus, the imaginary part of the computed field is located in the conductor.

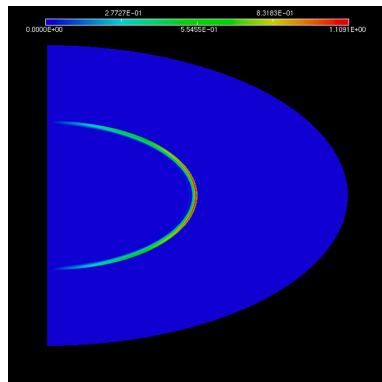
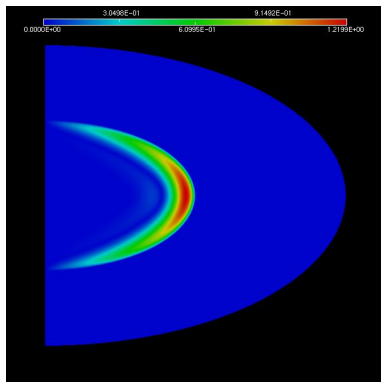


Figure: Configuration B. $|\operatorname{Im} H_\sigma|$ when $\sigma = 5$ and $\sigma = 80$

Skin effect in configuration A

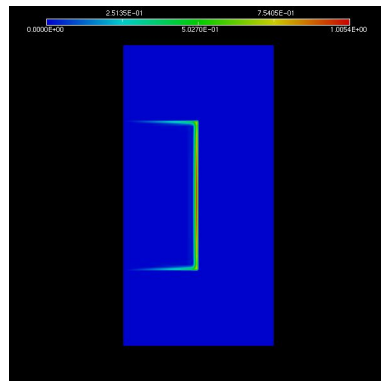
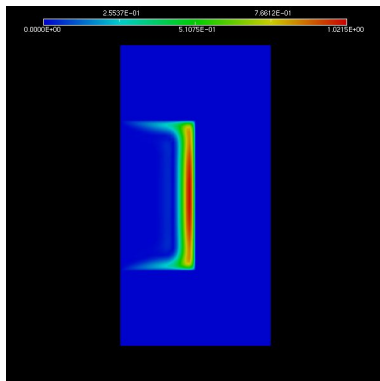


Figure: Configuration A. $|\text{Im } \mathbf{H}_\sigma|$ when $\sigma = 5$ and $\sigma = 80$

Influence of the Geometry on the Skin effect

Configuration B

$\mathcal{H} > 0$ on the left, and $\mathcal{H} < 0$ on the right

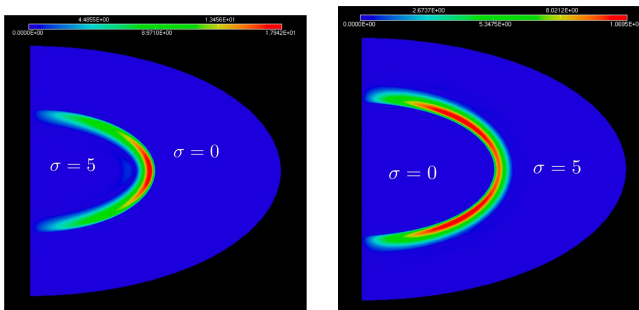


Figure: $|\operatorname{Im} H_\sigma|, \sigma = 5$

The skin depth is larger when the mean curvature of the conducting body surface is larger.

Outline

- 1 Framework
- 2 3D Multiscaled Asymptotic Expansion
- 3 Axisymmetric Problems
- 4 Finite Element Computations
- 5 Numerical simulations of skin effect
- 6 Postprocessing**

Configuration B

We perform numerical treatments from computations in configuration B.

We extract values of $\log_{10} |\mathbf{H}_\sigma|$ in Ω_-^m along the axis $z = 0 : y_3 = 2 - r$.

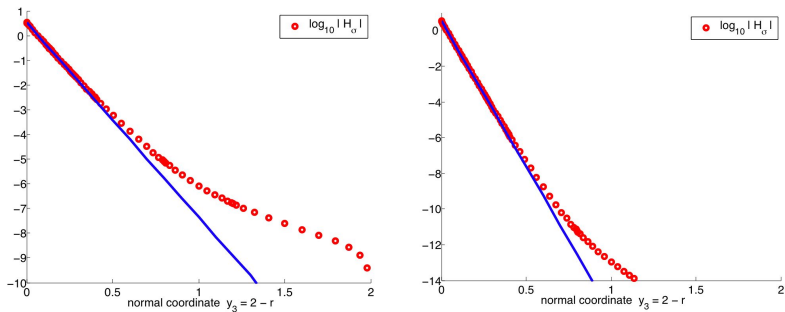
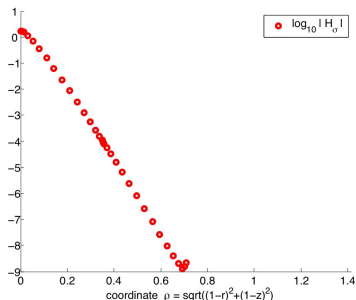
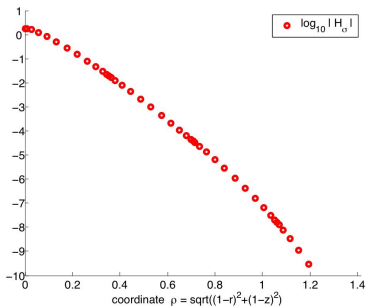


Figure: On the left $\sigma = 20$. On the right, $\sigma = 80$.

The curves exactly behave like lines: the exponential decay is obvious.

Configuration A

We extract values of $\log_{10} |H_\sigma|$ in Ω_-^m along the diagonal axis $r = z$



Here, $\rho = \sqrt{(1-r)^2 + (1-z)^2}$ is the distance to the corner point $\mathbf{a}(r = 1, z = 1)$.

The exponential decay is not obvious in configuration A.

To measure a possible exponential decay, we define the slopes

$$\tilde{s}_i(\sigma) := \frac{\log_{10} |\mathbf{H}_\sigma(r_i, z_i)| - \log_{10} |\mathbf{H}_\sigma(z_{i+1}, r_{i+1})|}{\rho_{i+1} - \rho_i}.$$

Here, $\rho_i := \sqrt{(1 - r_i)^2 + (1 - z_i)^2}$ is the distance from the extraction points (r_i, z_i) to \mathbf{a} .

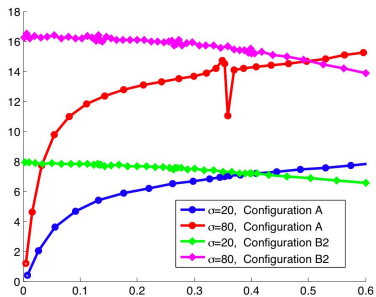


Figure: The graphs of the slopes $\tilde{s}_i(\sigma)$

Asymptotics in the conducting part

In configuration A, the slopes tend to 0, which means that there is no exponential convergence near the corner.

Nevertheless, a sort of exponential convergence is restored in a region further away from the corner.

The principal asymptotic contribution inside the conductor is a profile globally defined on a sector \mathcal{S} (of opening $\frac{\pi}{2}$) solving the model Dirichlet problem

$$\begin{cases} -i(\partial_X^2 + \partial_Y^2)v_0 + \kappa^2 v_0 = 0 & \text{in } \mathcal{S}, \\ v_0 = h_0^+(\mathbf{a}) & \text{on } \partial\mathcal{S}, \end{cases}$$

instead the 1D problem in configuration B

$$\begin{cases} -i\partial_Y^2 v_0 + \kappa^2 v_0 = 0 & \text{for } 0 < Y < +\infty, \\ v_0 = h_0^+ & \text{for } Y = 0. \end{cases}$$